Chemical Activation of Spent Diatomaceous Earth by Alkaline Etching in the Preparation of Mesoporous Adsorbents

Wen-Tien Tsai,* Kuo-Jong Hsien, and Chi-Wei Lai

Department of Environmental Engineering and Science, Chia Nan University of Pharmacy and Science, Tainan 717, Taiwan

This work was to study the activation regeneration of spent diatomaceous earth (SDE) for the preparation of mesoporous silica adsorbents by using alkaline activation method. Under the experimental conditions investigated, it was found that the alkaline activation method by sodium hydroxide under the controlled conditions significantly etched to proceed inwardly to the interior of the existing pore structure in the clay minerals, leaving a framework possessing a large Brunauer−Emmett−Teller surface area (over 100 m^2/g) and total pore volume (over 0.3 cm^3/g). The results indicated that these samples are type IV with a hysteresis loop. This observation was also in close agreement with the examinations on the scanning electron microscopy, X-ray diffraction, and Fourier transform infrared. Further, the adsorption rate of methylene blue onto the resulting clay adsorbent can be well described with the pseudo-second-order reaction model. The physical properties of the diatomaceous earth and resulting adsorbent were also consistent with the parameters obtained from the fittings of the common isotherms (Langmuir and Freundlich).

1. Introduction

Diatomaceous earth (DE) or diatomite typically consists of 86−94% silicon dioxide (SiO_2), with a significant quantity of alumina.[1] Because of its specific properties (i.e., high silica content, high porosity, low density, low conductivity coefficient, etc.), DE has been applied as a filter aid, adsorbent, filler, packing material for gas chromatography or high-performance liquid chromatography, insulator, catalyst (support), drilling-mud thickener, extender in paints, anticaking agent, natural insecticide, or grain protectant.[2−5] Spent DE (SDE), mainly generated from the food processing and distillery/brewery industries, is an industrial waste. In the past decades, the agroindustrial waste was commonly discarded in the field or simply disposed of as landfill without any pretreatment.[6] Taking into account the sustainable utilization of the mineral resource, SDE after activation regeneration as an adsorbent is very scarce in the literature. Leboda et al. reported that the waste bleaching earth containing DE and perlite from the food industry obtained in the process of apple juice purification was utilized for the preparation of carbon/mineral adsorbents.[7] They found that the pore properties of the carbon/mineral adsorbents obtained by the boiling (with continuous stirring) of the waste material for 5 h in an aqueous solution of sodium carbonate were significantly superior to those of the carbon/mineral adsorbents obtained by the direct pyrolysis and hydrothermal treatment methods.

Adsorption is generally considered to be an effective method for quickly lowering the concentration of the environmental organic compound in an effluent.[8−10] Recently, there is growing interest in utilizing low-cost wastes/alternatives to carbon adsorbent.[11−15] On the other hand, the unique property of activated carbon, in contrast to the other adsorbents, is that its surface is nonpolar or only slightly polar, which is not preferable to adsorb or remove polar organic molecules in the fluid streams.[16] Because of the negatively charged property in the surface, the clay adsorbent such as DE has been used for the removal of cationic or polar organic contaminants.[5,17−19]

This study was stimulated by the etching reaction between silica (i.e., SiO_2) and a strong base (e.g., NaOH).[20,21] The main objectives of this work were to study the feasibility of utilizing SDE as precursors in the production of mesoporous silica adsorbent and to further evaluate its adsorption properties for the removal of basic dye (i.e., methylene blue) from an aqueous solution at 25 °C.

2. Materials and Methods

2.1. Materials. The DE and its waste (i.e., SDE) were obtained from Shan-Hua Factory of Taiwan Tobacco & Liquor Co. (Tainan, Taiwan). The former was a calcined product (grade no. 577; Celite Corp., Santa Barbara, CA) with a median pore size of 14.0 μm examined by using a LS-230 laser diffraction particle size analyzer (Beckman Coulter, Inc., Fullerton, CA). The chemical compositions from the manufacturer's brochure mainly consist of 91.5% SiO_2, 4.0% Al_2O_3, and 1.1% Fe_2O_3. The latter was first dried in the oven for 48 h and then cooled to room temperature for further characterization and treatment. The carbon/hydrogen/nitrogen (C/H/N) contents of the dried waste sample were analyzed by using an elemental analyzer (model CHN-O-RAPID; Heraeus Sensor Technoloy GmbH, Kleinostheim, Germany), showing 0.82% (w/w) C, 0.29% (w/w) H, and 0.48% (w/w) N, which were obviously lower than those [i.e., 25.8% (w/w) C and 2.2% (w/w) H] reported by Leboda et al.[7] Sodium hydroxide (NaOH), which was purchased from Merck & Co., Inc. (Whitehouse Station, NJ), with ACS reagent grade, was selected as the chemical activator in this study to modify the SDE for the purposes of

* To whom correspondence should be addressed. Tel.: +886-6-2660393. Fax: +886-6-2669090. E-mail: wwtsai@mail.chna.edu.tw.

10.1021/ie0400651 CCC: $27.50
Published on Web 10/19/2004

removing residues left in that chemically create finer pores. The adsorbate used in the adsorption experiments was methylene blue (i.e., basic blue 9; CI 52015) with a minimum purity of 99% from Sigma Chemical Co. (St. Louis, MO).

2.2. Chemical Modification. Prior to the chemical modification with NaOH, the SDE was preliminarily tested with common strong acids (including sulfuric acid, phosphoric acid, hydrochloric acid, nitric acid, and acetic acid) to evaluate the usefulness of an increase of pore properties (i.e., specific surface area and/or pore volume) because the clay minerals were traditionally achieved by an acid activation method in which the acid penetration proceeded into the interior of the lattice structure from the edges, leaving a framework possessing a large area.[22−27] However, it was found in the study that the acid activation method had no profound influence on the pore structures compared to those of commercial DE, revealing that silicon dioxide in the frame structure of the SDE was quite unreactive during the acid treatment.

On the basis of the etching reaction between silica (i.e., SiO_2) and a strong base (i.e., NaOH), 5−25 g of the dried SDE was mixed with 100 mL of the NaOH solutions with various concentrations. Under holding times of 0.5−24.0 h and temperatures of 25−100 °C (boiling condition), the alkaline activation was carried out on a stirrer/hot plate with a boiler/reflux condenser. Afterward, the sample solution was filtered in a vacuum filter flask and washed sequentially with deionized water five times to remove the salt ions and other residues. The resulting solid was finally dried at 105 °C for 24 h and stored in a desiccator after drying.

2.3. Characterizations. The pore structures of DE, SDE, and NaOH-activated products relating to the surface area and pore volume were obtained by measuring their nitrogen adsorption/desorption isotherms at −196 °C in an ASAP 2010 apparatus (Micromeritics Co., Norcross, GA).[28] From the data of the total pore volume (V_t) and true (helium) density (ρ_s), the particle density (ρ_p), and porosity (ϵ_p) can be further obtained.[29,30] X-ray diffraction (XRD) was employed to observe the changes in crystallinity between the samples by using a Siemens D500 instrument (Cu Kα radiation). The surface pictures of the samples were made using scanning electron microscopy (SEM) by a JEOL JXA-840 (JEOL Ltd., Tokyo, Japan) apparatus. The ζ potentials of the samples were determined by a Zeta-Meter system 3.0 (Zeta-Meter Inc., Long Island City, NY) to obtain the charges at the surface of the mineral particles. Each data point was an average of at least five measurements. The Fourier transform infrared (FTIR) spectroscopy analysis has been used for the examination of functional groups on the surface of the samples. The spectrum was measured and recorded (500−2500 cm^{-1}) on a spectrometer (model DA 8.3; Bomen Co., Vanier, Quebec, Canada).

2.4. Adsorption Tests. Adsorption behaviors of the samples (including DE and an optimal activated solid) were tentatively determined to evaluate their potentials for the removal of methylene blue from an aqueous solution at 25.0 °C. All of the experiments of adsorption dynamics were carried out in a ca. 3-L stirred batch adsorber with four baffles, as similarly described in our previous studies.[31,32] In the present study, the adsorption solution was maintained at the same conditions (e.g., solution volume = 2 L and pH = 11.0) with an outer circulating water bath for the adsorbability of the basic dye under various initial concentrations. The concentration of the dye filtrate was measured immediately using a spectrophotometer (Hitachi UV-2001) at a λ_{max} of 661 nm. The amounts of methylene blue adsorbed onto the two adsorbents were determined as follows:

$$q_t = (C_0 - C_t)V/W \quad (1)$$

where C_0 and C_t are the initial and liquid-phase concentrations of a dye solution at t time (mg/L), respectively, V is the volume of the dye solution (ca. 2 L), and W is the mass of the dry adsorbent used (g).

Table 1. Main Physical Properties of DE and SDE

sample	S_{BET}[a] (m^2/g)	S_L[b] (m^2/g)	V_t[c] (cm^3/g)	ρ_s[d] (g/cm^3)	ρ_p[e] (g/cm^3)	ϵ_p[f]
DE	3.99	5.54	0.0065	2.256	2.223	0.0146
SDE	0.38	0.56	0.0039	2.413	2.391	0.0091

[a] BET surface area. [b] Langmuir surface area. [c] Total pore volume [d] True density. [e] Particle density, calculated by $\rho_p = 1/[V_t + (1/\rho_s)]$. [f] Particle porosity, computed by $\epsilon_p = 1 - (\rho_p/\rho_s)$.

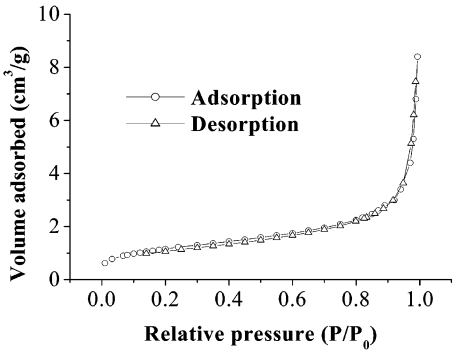

Figure 1. Nitrogen adsorption/desorption isotherms of DE.

3. Results and Discussion

3.1. Physical and Chemical Characterizations. The data in Table 1 indicate the Brunauer−Emmett−Teller (BET) and Langmuir surface areas, total pore volumes, densities, and porosities of the starting materials DE and SDE, revealing that these adsorbents possess poor pore properties toward the probe molecule (i.e., nitrogen). It will be expected that the desorption hysteresis loop does not occur practically on the N_2 isotherm, as shown in Figure 1. On the basis of the Brunauer, Deming, Deming, and Teller (BDDT) classification,[28] the adsorption isotherm belongs to a typical type II, which is most frequently encountered when adsorption occurs on nonporous materials or on materials with macropores or open voids.

It follows from the analysis (seen in Figure 2) of the BET surface area of the resulting solids prepared under a fixed holding time of 2 h and a solid/liquid ratio of 5 g/100 mL. In the NaOH-activated clay series, the rate of increase in the pore property at a NaOH concentration of 2.24 M is evidently faster than that at a NaOH concentration of 1.12 M. Also, the increase in the temperature from 60 to 100 °C tends toward pore development in the clay structure, resulting in an increase in the surface area. On the other hand, the effect of the activation time under an activation temperature of 80 °C and a solid/liquid ratio of 5 g/100 mL

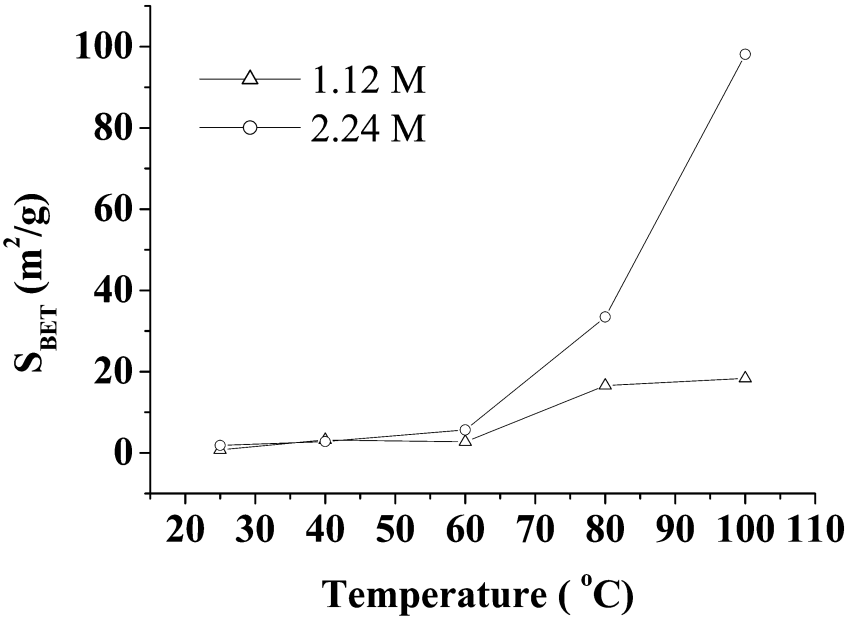

Figure 2. Effect of the activation temperature on BET surface areas of the resulting solid prepared at a NaOH concentration of 2.24 M, a fixed holding time of 2 h, and a solid/liquid ratio of 5 g/100 mL.

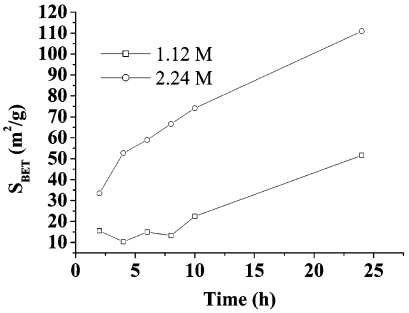

Figure 3. Effect of the holding time on BET surface areas of the resulting solid prepared at a NaOH concentration of 2.24 M, an activation temperature of 80 °C, and a solid/liquid ratio of 5 g/100 mL.

on the pore properties of the resulting solids is shown in Figure 3. It seems that the activation time plays a less important role in the production of the porous materials. It is seen that, with an increase in the activation time from 10 to 24 h at a NaOH concentration of 2.24 M, the BET surface areas of the resulting solids are only increased from 75 to 108 m^2/g as a result of the development of porosity. The pore properties were observed to increase gradually at a longer activation time, which should be due to the etching reaction in progress.

According to the data obtained from the preliminary experiments described above, the activation condition at an impregnation temperature of 100 °C (boiling) seems to have the most efficient effect on the development of pores. Table 2 lists the pore properties of the resulting products chemically activated from SDE at an activation time of 2 h and a solid/liquid ratio of 5 g/100 mL under various NaOH concentrations. In the moderate NaOH concentration range studied (i.e., 0.56−3.36 M), the pore properties (e.g., BET surface area) of the resulting solids basically increase with increasing NaOH concentration; i.e., ASDE-C1 (5.4 m^2/g) < ASDE-C2 (18.3 m^2/g) < ASDE-C3 (98.1 m^2/g). However, the values were observed to decrease gradually at a NaOH concentration of 3.36 M, which was possibly attributed to the rigorous reaction, resulting in the mesoporous pores

Table 2. Main Physical Properties of the Activated SDEs (ASDE Series) Produced with Various NaOH Concentrations[a]

sample id	NaOH concn (M)	S_{BET} (m^2/g)	S_L (m^2/g)	V_t (cm^3/g)	ρ_s (g/cm^3)	ρ_p (g/cm^3)	ϵ_p
ASDE-C1	0.56	5.4	8.9	0.018	2.540	2.429	0.044
ASDE-C2	1.12	18.3	31.1	0.060	2.545	2.208	0.132
ASDE-C3	2.24	98.1	165.8	0.258	2.731	1.602	0.413
ASDE-C4	3.36	72.6	147.4	0.229	2.954	1.762	0.404

[a] Prepared under the conditions of a temperature of ca. 100 °C (boiling), a holding time of 2 h, and a solid/liquid ratio of 5 g/100 mL.

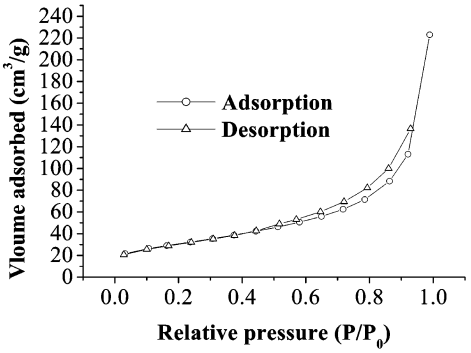

Figure 4. Nitrogen adsorption/desorption isotherms of the resulting solid (ASDE-t3).

produced being blocked by retained mineral and/or NaOH salt residues. In contrast to the data in Figure 3, it is noticeable that the pore property of the sample ASDE-C3 is close to that of the sample (denoted as ASDE-T80) produced at a NaOH concentration of 2.24 M, an activation temperature of 80 °C, and a holding time of 24 h, revealing that utilizing the boiling condition is an effective approach to decreasing the activation time in the production of mesoporous materials in the study. The nitrogen adsorption/desorption isotherm of the sample ASDE-C3 is shown in Figure 4. Compared with the above-described sample DE (Figure 1), a small hysteresis loop can be seen and closely connected with the interpretation of the type IV isotherm according to

Table 3. Main Physical Properties of the ASDE Series Produced with Various Activation Times[a]

sample id	activation time (h)	S_{BET} (m^2/g)	S_L (m^2/g)	V_t (cm^3/g)	ρ_s (g/cm^3)	ρ_p (g/cm^3)	ϵ_p
ASDE-t1	0.5	21.3	36.7	0.075	2.597	2.174	0.163
ASDE-t2	1.0	38.0	65.4	0.150	2.715	1.929	0.290
ASDE-t3[b]	2.0	98.1	165.8	0.258	2.731	1.602	0.413
ASDE-t4	4.0	108.9	184.0	0.344	2.829	1.434	0.493
ASDE-t3N[c]	2.0	10.8	21.5	0.068	2.729	2.302	0.156

[a] Prepared under the conditions of a temperature of ca. 100 °C (boiling), a holding time of 2 h, and a solid/liquid ratio of 5 g/100 mL. [b] The sample ASDE-C3 is identical with the sample ASDE-t3. [c] Washed with deionized water five times to remove the salt ions and other residues.

the BDDT classification. It is well-known that the type IV isotherms are characteristic of the mesoporous materials due to the nitrogen condensation.[28,30] The pore structures can be further deduced from certain shapes of the hysteresis loops. Clearly, the hysteresis loop of the sample ASDE-C3 corresponds to type H3 based on the recommendation of the International Union of Pure and Applied Chemistry (IUPAC),[28] which is associated with adsorbents having slit-shaped pores with wide mouths.[30]

The data in Table 3 list the pore properties of the ASDE series samples chemically activated from SDE at a NaOH concentration of 2.24 M. Generally, the pore properties of the resulting solids were observed to increase at higher activation time. However, it should be noted that an activation time of about 2 h was found to be optimal for higher pore properties presented in the study. As mentioned in the Experimental Section, after the chemical activation the crude products were subjected to washing with deionized water five times. It is known that washing with water removes the residues left in the resulting solids.[33] Thus, the final products obtained by washing will yield a well-developed porosity in the clay structure. This point had been confirmed in our previous study,[34] in which a corn cob was used as a precursor to prepare activated carbon by employing the combined activation. The test was performed on the samples ASDE-t3 and ASDE-t3N. The results of pore properties before and after washing of the samples are also presented in Table 3. The results clearly show that about 90% of porosity (reflected by the BET surface area) created in the clay sample was occupied by salts and/or residues in the structure. The small surface area of the unwashed clay sample is because of salts and/or residues left in the products, blocking pore entrances to the nitrogen molecules based on the analysis of adsorption and desorption isotherms of nitrogen for determining the BET surface area. The foregoing results may be further observed in the pore size distribution curves based on the pore volumes of the Barrett−Joyner−Halenda desorption branch in the measurement of N_2 isotherms,[28] as shown in Figure 5. It is seen that the pores of these clay samples (including ASDE-t1, ASDE-t2, ASDE-t3, and ASDE-t4), in particular ASDE-t3, have a heterogeneous distribution of pore diameters with major pore ranges below about 15 nm, which may be useful for their possible applications in adsorption from the liquid phase.

To study the substantial influence of the solid/liquid ratio on the porosity development, the chemical activations of SDE impregnated with a 2.24 M NaOH solution were carried out at a temperature of 100 °C (boiling) and an activation time of 2 h under various dosages of SDE. As shown in Figure 6, the BET surface areas of the resulting solids tend toward a gradual decrease with an increase in the dosage ranging from 5 to 25 g/100 mL. The decrease in the pore property is clearly due to a lower etching rate of the reaction at a higher solid/liquid ratio.

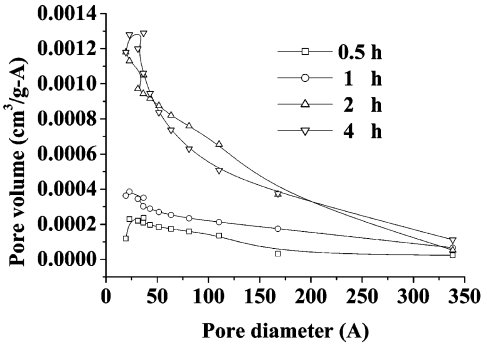

Figure 5. Pore size distributions of the resulting solids.

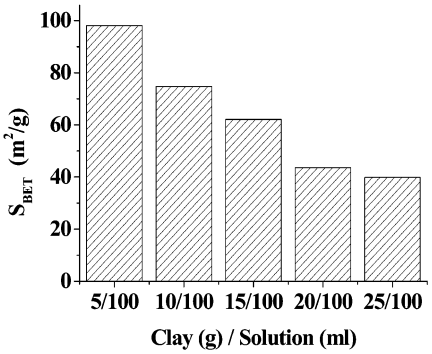

Figure 6. Effect of the solid/liquid ratio on BET surface areas of the resulting solid prepared at a NaOH concentration of 2.24 M, an activation temperature of 100 °C (boiling), and a holding time of 2 h.

SEM micrographs of the surface structures of some typical samples (including DE, SDE, ASDE-T80, and ASDE-t3) are illustrated in Figure 7, showing a great difference between these samples. The porous structure examination of the precursors DE and SDE can be clearly seen in the SEM photographs (parts a and b of Figure 7, respectively), revealing the variety of shapes and macropores/open voids that give the DEs a high ability to trap solids or residues for separation from clear liquids. However, the pores can be developed and further enhanced by chemical activation during the etching reaction by NaOH, which results in the formation of some pores, as illustrated in Figure 7c,d. The sample ASDE-t3 displays a much more rough and irregular surface structure, indicating a gross attack on the exterior surface and interior pore wall. As a result, it effectively creates new pores and increases the pore properties as listed in Table 3 and shown in Figure 5.

To observe changes in the crystallinity as a result of the NaOH activation, the powder XRD patterns of some typical samples (including DE, SDE, ASDE-T80, and

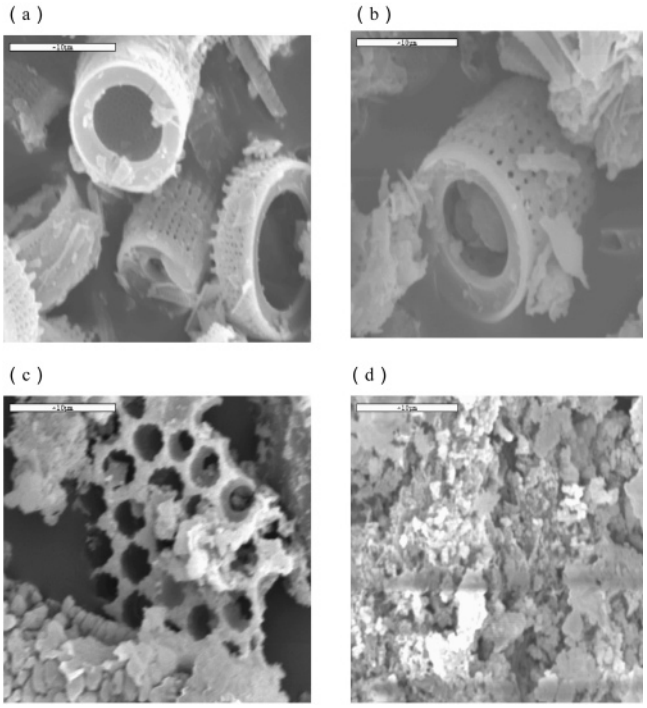

Figure 7. SEM photographs of the starting solids (DE and SDE) and the resulting activated solids (ASDE-T80 and ASDE-t3).

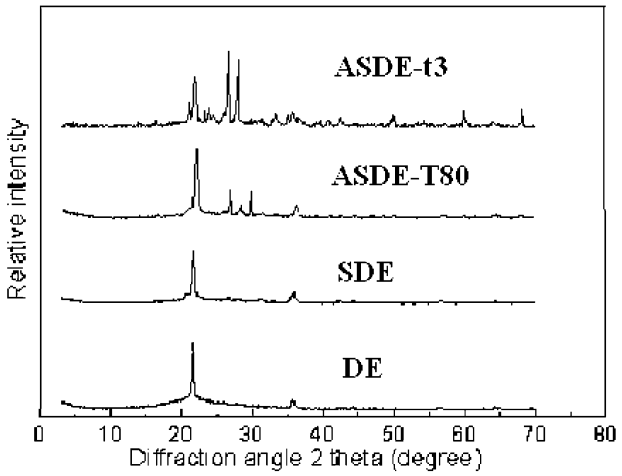

Figure 8. XRD diffractograms of the starting solids (DE and SDE) and the resulting activated solids (ASDE-T80 and ASDE-t3).

ASDE-t3) are shown in Figure 8. Although all of the crystalline phases belonging to the main components (e.g., silica) are clearly visible, the relative intensity can be served to elucidate the effects of the activation procedure employed on phase crystallinity. The XRD patterns in Figure 8 indicate the gradual deterioration and disappearance of the silica peaks. This phenomenon may be interpreted in terms of the etching action of NaOH on silica. In this regard, the degradation of the layered structure is indicated by the progressive loss in the peak intensity of the silica peaks as the severity of NaOH activation increases, showing that the resulting sample ASDE-t3 has a lower resistance to NaOH attack, and its pore property is thus enhanced at the boiling activation conditions. For example, the intensity ratio of ASDE-t3 to ASDE-T80 at the silica peak (2θ = 21.6−22.0) is only 30%. Similar results on acid-activated clays have been recorded in the literature.[35−39] It was also found from Figure 8 that the XRD of the samples

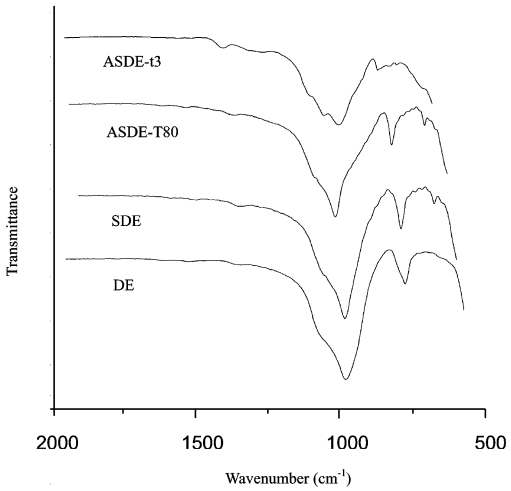

Figure 9. FTIR spectra of the starting solids (DE and SDE) and the resulting activated solids (ASDE-T80 and ASDE-t3).

ASDE-T80 and ASDE-t3 exhibits some lines of reflections at 2θ of 25−30°, which are indicative of the probable presence of extraneous impurities such as calcite, quartz, and feldspar.[36]

In the series activated with NaOH, the loss of crystallinity and the appearance of amorphous silica were also observed in the FTIR spectra of the samples DE, SDE, ASDE-T80, and ASDE-t3 displayed in Figure 9. Clearly, characteristic bands due to silicate structure are seen between 1400 and 400 cm^{-1}. Some significant differences between the natural and activated solids can be observed, mainly those corresponding to Si−O bonds in the tetrahedral sheet. The wide bands centered at ca. 1090 cm^{-1} should be due to Si−O−Si in-plane vibration (asymmetric stretching).[35,38] Also, the progressive broadening of the band when NaOH etching attack progresses indicates that the structures of the resulting solids become more and more amorphous, which is significantly consistent with the results on the morphology of the underlying clay structure from the SEM (Figure 7) and XRD (Figure 8). Similar observations can be seen for the band centered at ca. 795 cm^{-1}, which is also characteristic of silica. Again, the intensity of the band obviously decreases with NaOH activation. This may be attributed to the progressive leaching or removal of silicon cations owing to the alkaline etching as described above.

It is well-known that clays are effective natural adsorbents because of their lamellar structures and negatively charged surfaces, which make them good cation adsorbents by ion exchange. The surface charges (denoted as the ξ potential) of the DE may arise from their functional groups at the surface such as −OH.[18] Figure 10 shows the ξ potential values of the samples SDE and ASDE-t3 as a function of pH. As an analytical comparison, the reference sample silicate was also carried out in this study. As shown in Figure 10, the surface charge decreases as the pH increases. It is noted that, as the pH is increased, the surface hydroxides lose their protons in response to the increasing number of negatively charged sites. Thus, the surface of the activated clay at the experimental conditions (i.e., pH > 3.0) will exhibit negative charges mainly because of the variable charge from pH-dependent surface hydroxyl sites. From the data of the ζ potential vs pH, the isoelectric point or pH of the point of zero charge (i.e., pH_{pzc}) of the clay/water system was thus determined to

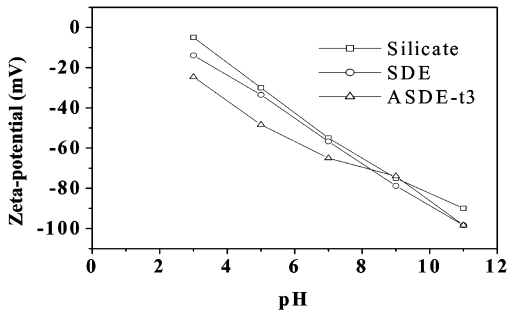

Figure 10. Plots of ξ potential vs pH of the starting solid (SDE) and the resulting activated solid (ASDE-t3).

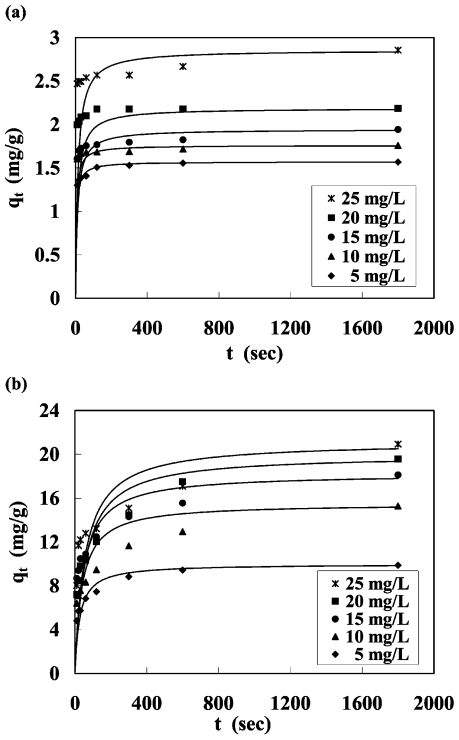

Figure 11. Pseudo-second-order adsorption kinetics of methylene blue onto (a) DE and (b) ASDE-t3 adsorbents with dosages of 5 g/2 L and 1.0 g/2 L, respectively. Adsorption conditions: initial concentrations = 5−25 mg/dm^3, temperature = 25 °C, pH = 7.0, and agitation speed = 400 rpm. Symbols: experimental data. Full lines: calculated from eq 2 and Table 4.

be about 2.0, which is very close to the pH_{pzc} values of silicon dioxide at 2.0 and montmorillonite at 2.5.[40]

3.2. Adsorption Properties. In the adsorption experiments, the resulting solid ASDE-t3 and the starting material DE were chosen as adsorbents. The adsorption test revealed that the rate of adsorption of the cationic dye onto the clay adsorbent was extremely fast and quickly approached a plateau, showing considerable significance in the ion-exchange process. The effect of the initial dye concentration on the adsorption intake of methylene blue at an initial pH of 7.0, a temperature of 25 °C, and a mixing speed of 400 rpm is shown in Figure 11, where the experimental data are indicated as discrete points and those thus obtained from the pseudo-second-order kinetic model by solid lines, as described with its linear form[31,32,41]

$$t/q_t = 1/(kq_e^2) + (1/q_e)t \qquad (2)$$

where k is the pseudo-second-order rate constant (g/mg·min), q_e is the amount of methylene blue adsorbed at equilibrium (mg/g), and q_t is the amount of methylene blue adsorbed at time t (mg/g). Rate parameters k and q_e can be directly obtained from the intercept and slope of the plot of t/q_t vs t. Values of k and q, computed from eq 2, are listed in Table 4. It is clear that the kinetics of methylene blue adsorption on the NaOH-activated adsorbent follows this model with regression coefficients of higher than 0.99 for all of the systems in this study. Also, the adsorption capacity (i.e., q_e) indicates an increase with the initial concentration of methylene blue.

Table 4. Kinetic Parameters for Methylene Blue Adsorption onto DE and ASDE-t3 at 25 °C

adsorbent	C_0 (mg/L)	k (g/mg·min)	q_e (mg/g)	correlation coefficient	C_e (mg/L)
DE[a]	5	0.130	1.571	1.0000	1.073
	10	0.113	1.758	0.9999	5.604
	15	0.045	1.943	0.9995	10.142
	20	0.307	2.187	1.0000	14.533
	25	0.026	2.856	0.9993	17.859
ASDE-t3[b]	5	0.0038	9.990	0.9997	0.005
	10	0.0012	15.504	0.9960	2.248
	15	0.0012	18.315	0.9968	5.843
	20	0.0009	19.960	0.9970	10.020
	25	0.0009	21.142	0.9933	14.429

[a] Adsorption conditions: adsorbent dosage = 5 g/2.0 L^1, agitation speed = 400 rpm, pH = 7, and temperature = 25 °C. [b] Adsorption conditions: adsorbent dosage = 1 g/2.0 L^1, agitation speed = 400 rpm, pH = 7, and temperature = 25 °C.

Table 5. Parameters in Langmuir and Freundlich Isotherm Models of Methylene Blue onto DE and ASDE-t3 at 25 °C

	Langmuir			Freundlich		
adsorbent	q_m (mg/g)	K_L (L/mg)	R^2	K_F [mg/g (L/mg)$^{1/n}$]	$1/n$	R^2
DE	2.24	2.1	0.5577	1.45	0.17	0.7042
ASDE-t3	18.48	270.5	0.9093	15.78	0.09	0.9666

Two common isotherm equations have been applied to model the isotherms in the present study: Langmuir and Freundlich models.[8,41]

$$\text{Langmuir:}\quad 1/q_e = 1/[(K_L q_m)C_e] + 1/q_m \qquad (3)$$

$$\text{Freundlich:}\quad q_e = K_F C_e^{1/n} \qquad (4)$$

In eq 3, C_e and q_e are the concentration (mg/L) and amount (mg/g) of methylene blue adsorbed at equilibrium, respectively, K_L is a direct measure for the intensity of the adsorption process (L/mg), and q_m is a constant related to the area occupied by a monolayer of the absorbate, reflecting the adsorption capacity (mg/g). From a plot of $1/q_e$ vs $1/C_e$, q_m and K_L can be determined from its slope and intercept. In eq 4, K_F is a constant for the system, related to the bonding energy. K_F can be defined as the adsorption or distribution coefficient and represents the quantity of dye adsorbed onto adsorbents for a unit equilibrium concentration (i.e., C_e = 1 mg/dm^3). The slope $1/n$, ranging between 0 and 1, is a measure of the adsorption intensity or surface heterogeneity.

Table 5 presents the results of Langmuir and Freundlich isotherm fits by using the adsorption capacity data at 25 °C. Obviously, it can be seen that the Freundlich model yields a somewhat better fit than the Langmuir model, as reflected with correlation coefficients (R^2). The adsorption isotherms revealed that the activated clay adsorbent can quickly uptake 18.5 mg/g in a relatively

low concentration of the basic dye in an aqueous medium. As is also illustrated in Table 5, the value of $1/n$ is far below 1.0, which indicates a favorable adsorption isotherm. It was further found that the determined parameters of the isotherm equations were highly consistent with the pore properties of these two adsorbents as listed in Tables 1 and 3. The maximum adsorption capacity of methylene blue, q_m, was much higher than that of other potential adsorbents such as fly ash and zeolite. [42]

4. Conclusions

In conclusion, the etching treatment of SDE changes the surface properties by using alkaline activation methods. The porosities of the resulting solids thus obtained in the study are over 0.4, indicating that these samples are type IV with a hysteresis loop corresponding to type H3 from nitrogen isotherms. This observation was also in close agreement with the results of SEM, XRD, and FTIR. In contrast, the optimal mesoporous material thus prepared and the starting material (i.e., DE) were used as mineral adsorbents for adsorption of methylene blue (basic dye 9) at 25 °C. The adsorption kinetics of methylene blue under various initial dye concentrations can be well described with the pseudo-second-order reaction model. The physical properties of the two adsorbents were consistent with the parameters obtained from the fittings of the common isotherms.

Acknowledgment

This research was supported by National Science Council (NSC), Taipei, Taiwan, under Contract NSC 92-2211-E-041-009.

Literature Cited

(1) Engh, K. R. Diatomite. In *Kirk−Othmer Encyclopedia of Chemical Technology*, 4th ed.; Howe-Grant, M., Ed.; John Wiley & Sons: New York, 1993; Vol. 8, p 108.

(2) Manning, D. A. C. *Introduction to Industrial Minerals*; Chapman & Hall: London, 1995.

(3) Lemonas, J. F. Diatomite. *Am. Ceram. Soc. Bull.* **1997**, *76* (6), 92.

(4) Korunic, Z. Review: Diatomaceous Earths, a Group of Natural Insecticides. *J. Stored Prod. Res.* **1998**, *34*, 87.

(5) Agdi, K.; Bouaid, A.; Martin Esteban, A.; Fernandez Hernando, P.; Azmani, A.; Camara, C. Removal of Atrazine and four Organophosphorus Pesticides from Environmental Waters by Diatomaceous Earth-Remediation Method. *J. Environ. Monit.* **2000**, *2*, 420.

(6) Wei, M. S.; Huang, K. H. Recycling and Reuse of Industrial Wastes in Taiwan. *Waste Manage.* **2001**, *21*, 93.

(7) Leboda, R.; Skubiszewska-Zieba, J.; Charmas, B.; Chodorowski, S.; Pokrovskiy, V. A. Carbon−Mineral Adsorbents from Waste Materials: Case Study. *J. Colloid Interface Sci.* **2003**, *259*, 1.

(8) Noll, K. E.; Gounaris, V.; Hou, W. S. *Adsorption Technology for Air and Water Pollution Control*; Lewis: Chelsea, MI, 1992.

(9) Al Duri, B. Introduction to Adsorption. In *Use of Adsorbents for the Removal of Pollutants from Wastewaters*; McKay, G., Ed.; CRC Press: Boca Raton, FL, 1996.

(10) Reife, A.; Freeman, H. S. Carbon Adsorption of Dyes and Selected Intermediates. In *Environmental Chemistry of Dyes and Pigments*; Reife, A., Freeman, H. S., Eds.; John Wiley & Sons: New York; 1996.

(11) Pollard, S. J. T.; Fowler, G. D.; Sollars, C. J.; Perry, R. Low-Cost Adsorbents for Waste and Wastewater Treatment: a Review. *Sci. Total Environ.* **1992**, *116*, 31.

(12) Allen, S. J. Types of Adsorbent Materials. In *Use of Adsorbents for the Removal of Pollutants from Wastewaters*; McKay, G., Ed.; CRC Press: Boca Raton, FL, 1996.

(13) Ramakrishna, K. R.; Viraraghavan, T. Dye Removal Using Low Cost Adsorbents. *Water Sci. Technol.* **1997**, *36* (2−3), 189.

(14) Bailey, S. E.; Olin, T. J.; Bricka, R. M.; Adrian, D. D. A Review of Potentially Low-Cost Sorbents for Heavy Metals. *Water Res.* **1999**, *33*, 2469.

(15) Gupta, V. K.; Ali, I. Adsorbents for Water Treatment: Low-Cost Alternatives to Carbon. In *Encyclopedia of Surface and Colloid Science*; Hubbard, A. T., Ed.; Marcel Dekker: New York, 2002.

(16) Yang, R. T. *Gas Separation by Adsorption Processes*; Butterworth: Boston, 1987.

(17) Lin, S. H. Adsorption of Disperse Dye by Various Adsorbents. *J. Chem. Technol. Biotechnol.* **1993**, *58*, 159.

(18) Al-Ghouti, M. A.; Khraisheh, M. A. M.; Allen, S. J.; Ahmad, M. N. The Removal of Dyes from Textile Wastewater: a Study of the Physical Characteristics and Adsorption Mechanisms of Diatomaceous Earth. *J. Environ. Manage.* **2003**, *69*, 229.

(19) Shawabkeh, R. A.; Tutunji, M. F. Experimental Study and Modeling of Basic Dye Sorption by Diatomaceous Clay. *Appl. Clay Sci.* **2003**, *24*, 111.

(20) Miller, F. M. *Chemistry: Structure and Dynamics*; McGraw-Hill: New York, 1984.

(21) Hawkinson, T. E.; Korpela, D. B. Chemical Hazards in Semiconductor Operations. In *Semiconductor Safety Handbook: Safety and Health in the Semiconductor Industry*; Bolmen, R. A., Jr., Ed.; Noyes: Westwood, NJ, 1997.

(22) Hasnuddin Siddiqui, M. K. *Bleaching Earths*; Pergamon: London, 1968.

(23) Vicente-Rodriguez, M. A.; Suarez, M.; Banares-Munoz, M. A.; Lopez-Gonzalez, J. D. Comparative FT-IR Study of the Removal of Octahedral Cations and Structural Modifications during Acid Treatment of Several Silicates. *Spectrochim. Acta, Part A* **1996**, *52*, 1685.

(24) Kooli, F.; Jones, W. Characterization and Catalytic Properties of a Saponite Clay Modified by Acid Activation. *Clay Miner.* **1997**, *32*, 633.

(25) Mahmoud, S.; Saleh, S. Effect of Acid Activation on the De-*tert*-butylation Activity of Some Jordanian Clays. *Clays Clay Miner.* **1999**, *47*, 481.

(26) Kurama, H.; Zimmer, A.; Reschetilowski, W. Chemical Modification Effect on the Sorption Capacities of Natural Clinoptilolite. *Chem. Eng. Technol.* **2002**, *25*, 301.

(27) Espantaleon, A. G.; Nieto, J. A.; Fernandez, M.; Marsal, A. Use of Activated Clays in the Removal of Dyes and Surfactants from Tannery Wastewaters. *Appl. Clay Sci.* **2003**, *24*, 105.

(28) Gregg, S. J.; Sing, K. S. W. *Adsorption, Surface Area and Porosity*, 2nd ed.; Academic Press: London, 1982.

(29) Smith, J. M. *Chemical Engineering Kinetics*, 3rd ed.; McGraw-Hill: New York, 1981.

(30) Richardson, J. T. *Principles of Catalyst Development*; Plenum Press: New York, 1989.

(31) Tsai, W. T.; Lai, C. W.; Hsien, K. J. Effect of Particle Size of Activated Clay on the Adsorption of Paraquat from Aqueous Solution. *J. Colloid Interface Sci.* **2003**, *263*, 29.

(32) Tsai, W. T.; Lai, C. W.; Hsien, K. The Effects of pH and Salinity on Kinetics of Paraquat Sorption onto Activated Clay J. *Colloids Surf. A* **2003**, *224*, 99.

(33) Ahmadpour, A.; Do, D. D. The Preparation of Active Carbons from Coal by Chemical and Physical Activation. *Carbon* **1996**, *34*, 471.

(34) Tsai, W. T.; Chang, C. Y.; Wang, S. Y.; Chang, C. F.; Chien, S. F.; Sun, H. F. Preparation of Activated Carbons from Corn Cob Catalyzed by Potassium Salts and Subsequent Gasification with CO_2. *Bioresour. Technol.* **2001**, *78*, 203.

(35) Vicente Rodriguez, M. A.; Suarez Barrios, M.; Lopez Gonzalez, J. D.; Banares Munoz, M. A. Acid Activation of a Ferrous Saponite (Griffithite): Physico-Chemical Characterization and Surface Area of the Products Obtained. *Clays Clay Miner.* **1994**, *42*, 724.

(36) Bovey, J.; Jones, W. Characterization of Al-Pillared Acid Activated Clay Catalysts. *J. Mater. Chem.* **1995**, *5*, 2027.

(37) Kumar, P.; Jasra, R. V.; Bhat, T. S. G. Evolution of Porosity and Surface Acidity in Montmorillonite Clay on Acid Activation. *Ind. Eng. Chem. Res.* **1995**, *34*, 1440.

(38) Falaras, P.; Kovanis, I.; Lezou, F.; Seiragakis, G. Cottonseed Oil Bleaching by Acid-activated Montmorillonite. *Clay Miner.* **1999**, *34*, 221.

(39) Falaras, P.; Lezou, F.; Seiragakis, G.; Petrakis, D. Bleaching Properties of Alumina-Pillared Acid-activated Montmorillonite. *Clays Clay Miner.* **2000**, *48*, 549.

(40) Evangelou, V. P. *Environmental Soil and Water Chemistry: Principles and Applications*; John Wiley & Sons: New York, 1998.

(41) Reddad, Z.; Gerente, C.; Andres, Y.; Le Cloirec, P. Adsorption of Several Metal Ions onto a Low-Cost Biosorbent: Kinetic and Equilibrium Studies. *Environ. Sci. Technol.* **2002**, *36*, 2067.

(42) Banat, F.; Al-Asheh, S.; Al-Makhadmeh, L. Evaluation of the Use of Raw and Activated Date Pits as Potential Adsorbents for Dye Containing Waters. *Process Biochem*. **2003**, *39*, 193.

Received for review February 27, 2004
Revised manuscript received September 1, 2004
Accepted September 2, 2004

IE0400651